This article was downloaded by:
On: *15 January 2011*
Access details: *Access Details: Free Access*
Publisher *Taylor & Francis*
Informa Ltd Registered in England and Wales Registered Number: 1072954 Registered office: Mortimer House, 37-41 Mortimer Street, London W1T 3JH, UK

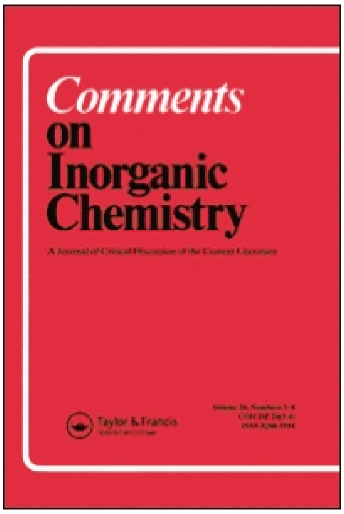

Comments on Inorganic Chemistry
Publication details, including instructions for authors and subscription information:
http://www.informaworld.com/smpp/title~content=t713455155

Zeolites and Intrazeolite Chemistry: Insights from Infrared Spectroscopy

C. Otero Areán[a]
[a] Departamento de Quimica, Universidad de las Islas Baleares, Spain

To cite this Article Areán, C. Otero(2000) 'Zeolites and Intrazeolite Chemistry: Insights from Infrared Spectroscopy', Comments on Inorganic Chemistry, 22: 3, 241 — 273

To link to this Article: DOI: 10.1080/02603590008050871

URL: http://dx.doi.org/10.1080/02603590008050871

PLEASE SCROLL DOWN FOR ARTICLE

Full terms and conditions of use: http://www.informaworld.com/terms-and-conditions-of-access.pdf

This article may be used for research, teaching and private study purposes. Any substantial or systematic reproduction, re-distribution, re-selling, loan or sub-licensing, systematic supply or distribution in any form to anyone is expressly forbidden.

The publisher does not give any warranty express or implied or make any representation that the contents will be complete or accurate or up to date. The accuracy of any instructions, formulae and drug doses should be independently verified with primary sources. The publisher shall not be liable for any loss, actions, claims, proceedings, demand or costs or damages whatsoever or howsoever caused arising directly or indirectly in connection with or arising out of the use of this material.

Zeolites and Intrazeolite Chemistry: Insights from Infrared Spectroscopy

C. OTERO AREÁN*
Departamento de Química,
Universidad de las Islas Baleares,
07071 Palma de Mallorca, Spain

(Received May 05, 2000)

Downloaded At: 12:22 15 January 2011

Zeolites are widely used as adsorbents, catalysts, ion exchangers and molecular sieves. However, less is known about the potential use of zeolites and related microporous solids for tailored synthesis of advanced materials. Zeolite-based host-guest nanocomposites are a type of advanced material in which zeolites act as hosts for encapsulating and organizing molecules, crystalline nano-phases and supramolecular entities inside the zeolite pores. Space confinement and host-guest (electrostatic) interaction results in composite materials possessing novel optical, electronic and magnetic properties. Potential technological applications can be expected in a number of fields, such as chemical and biological sensing, semiconductor devices and photonics, to name only a few examples. A related aspect is the fine tuning of the intracrystalline space in zeolites for controlling intrazeolite chemical processes, including the conversion of zeolite cavities into chiral chambers which act as very selective catalysts for the asymmetric synthesis of fine chemicals. Developments in all of these fields critically depend upon improved methods for zeolite characterization and for studying intrazeolite chemistry. For both of these purposes many instrumental techniques are currently being used. Among them, IR spectroscopy deserves special attention. Recent advances in IR spectroscopy of zeolites include the use of variable temperature procedures, synchrotron IR radiation and ultrafast time-resolved IR spectrometry. Examples are given of how IR spectroscopy is strongly contributing to an improved

---

* Corresponding Author.

Comments Inorg. Chem.
2000, Vol. 22, No. 3-4, pp. 241-273
Reprints available directly from the publisher
Photocopying permitted by license only

© 2000 OPA (Overseas Publishers Association)
Amsterdam N.V. Published by license
under the Gordon and Breach
Science Publishers imprint.
Printed in Malaysia

understanding of zeolites and intrazeolite chemistry, which is needed in order to extend potential applications of zeolite-based materials.

Keywords: *advanced materials; infrared spectroscopy; intrazeolite chemistry; nanocomposites; zeolite-based materials; zeolites*

1. INTRODUCTION

Zeolites are three-dimensional aluminosilicates (tectosilicates) formed by corner sharing $SiO_4$and AlO_4 tetrahedral units. The framework thus formed has a negative electric charge which has to be balanced by extra-framework cations or protons. These charge balancing ions, which can easily be exchanged, are responsible for some important properties of zeolites; such as Brønsted acidity, adsorption potential and intrazeolite electric fields. Other useful properties are more directly related to framework composition (Si:Al ratio), pore size and connectivity.

The zeolite framework encloses open channels and cavities (up to 50% of the total volume) which show a characteristic, and regular, spatial arrangement and dimensions for each particular structure type.[1] Zeolites can thus be regarded as being the archetype of periodic microporous systems, as opposed to non-periodic porous materials such as active carbon, xerogels and aerogels. Regular pore size endows zeolites with their potential to act as molecular sieves and size-selective catalysts. Periodicity of pore layout can lead to formation of superstructures in zeolite based host-guest composites; a new generation of advanced materials which offers a range of properties and uses that are only just beginning to be explored, as the number and versatility of structure types is being increased.

Aluminosilicate zeolites (both natural and synthetic) were the main class of microporous materials known in the 1950s, but many other open framework crystalline structures are now known, and their number is rapidly increasing. In the early 1980s the synthesis of non-siliceous periodic microporous solids (such as aluminophosphates) was achieved, and during the late 1980s and the 1990s the range of chemical composition was expanded to include germanates, oxofluorides, sulfides and nitrides, as well as purely siliceous materials such as silicalite and the MCM series of periodic mesoporous structures.[2–5] The rich diversity of chemical composition was also increased by partial isomorphous substitution of framework Si or Al atoms by other elements. Examples are B,

Downloaded At: 12:22 15 January 2011

Ga, Fe or Ti, but actually more than 20 elements (both from the main groups and the transition series) can now be incorporated into zeotype frameworks; zeotypes are materials which have variable chemical composition while retaining a zeolite-type structure. The range of periodic porous solids has also increased on the structural ground. Many of the new architectures involve structural units other than XO_4 tetrahedra, such as octahedral XO_6, pyramidal XO_4, or pentacoordinated XO_5 units.

Versatile chemical composition and framework topology results in a large variety of microporous and mesoporous materials, including zeolites and zeotypes, having a wide scope of potential usage. Classical applications of zeolites include their use as heterogeneous catalysts (mainly in the petrochemical industry), as adsorbents and ion exchangers, and as detergent builders. These applications account for most of the current commercial production of zeolites, which is of about 1.6 million tonnes per year. New areas of technological development include the use of zeolites as ultraselective catalysts (for pollution control and the synthesis of fine chemicals), tailored host-guest materials for application in electronic, optical or magnetic devices, and also clever design of chemical sensors, transducers and modified membranes.[6–9] A summary of main applications of zeolites, both actual and prospective, is given in Table I.

TABLE I Some main applications of zeolites and zeotypes

Actual uses

Adsorbents and molecular sieves:

- drying agents (water vapour removal)
- air separation (nitrogen from oxygen)
- sulphur removal (*e.g.* from natural gas)
- separations based on sieving and selectivity

Ion exchangers:

- water softeners and purifiers
- detergent builders
- metal separation (removal form waste water)
- radioisotope removal and storage

Downloaded At: 12:22 15 January 2011

- ion exchange fertilizers
- ruminant feeding (non-protein nitrogen)
- aquaculture (removal)
- artificial kidney dialysate regeneration

Catalysts:

- fluid cracking (gasoline production)
- shape-selective reforming
- methanol to gasoline conversion
- hydrogenation, dehydrogenation and hydrodealkylation
- xylene isomerisation (polyester polymers)
- phenol to hydroquinone conversion
- pollution control (DeNOx reactions)
- synthesis of speciality chemicals

Future possibilities

Stereoselective catalytic processes

Nanoreactors (fine control over intrazeolite chemical processes by tuning physico-chemical properties of intrazeolite cavities and channels)

Affinity chromatography and immunosorption assays

Selective membranes

Selective electrodes

Nano-composites for electro-opticals

Nano-composites having hierarchical structures (superstructures)

Tailored (quantum-sized) semiconductors

Size-controlled magnetic materials

Encapsulated conducting polymers

Encapsulated photosensitive dyes (light-energy harvesting and non-linear optics)

Encapsulated luminescent centres (Mn^{2+}, lanthanides)

Chemical and biomedical sensors (including encapsulated sensing species)

Contrast enhancement agents (*e.g.* for MRI)

Downloaded At: 12:22 15 January 2011

Some potential applications of zeolite-based materials stem from the regular arrangement and variable connectivity of zeolite pores and cages, which afford a means for controlled assembly of a superlattice of electronic, optical or magnetic materials having one or more dimensions in the nanometer range. This is a range where quantum size effects give rise to useful macroscopic properties. However, it is also the length scale where our ability to synthesize materials is weakest. Intrazeolite synthesis provides the synthetic chemist with a means to overcome the thermodynamic tendency of larger particles to grow at the expense of smaller ones, thus furnishing a route for the preparation of nano-structured materials. From a different perspective, fine tuning of relevant physico-chemical properties of the intrazeolite space should lead to an extended control over a wide range of chemical processes mediated by zeolites, allowing these structures to be used as cleverly designed nano-reactors.

Downloaded At: 12:22 15 January 2011

2. OVERVIEW OF ZEOLITE TOPOLOGY

In the early 1950s, when systematic research on zeolites was started,[10–12] only six structure types were known. This number has now been raised to well over one hundred and it continues to grow at a brisk pace, mainly by steady incorporation of new synthetic materials. Structure types, which are named with a code consisting of three capital letters, do not depend on chemical composition, distribution of framework atoms (T-atoms) or crystal symmetry. They simply denote the topology of a zeolite-type framework, *i.e.*, the way (connectivity) in which structural units (TO_4 tetrahedra) are arranged. This connectivity determines pore size, shape and dimensionality. The number of T-atoms that define the pore openings (ring size) is an important structural parameter. Zeolites containing rings consisting of 8, 10 and 12 T-atoms are denoted as small-, medium- and large-pore materials. The corresponding pore openings are about 0.4, 0.55 and 0.74 nm in size, respectively. However, zeotypes containing larger rings have also been synthetized, and siliceous materials belonging to the MCM series possess channel diameters in the 2–5 nm range, or even larger.

Downloaded At: 12:22 15 January 2011

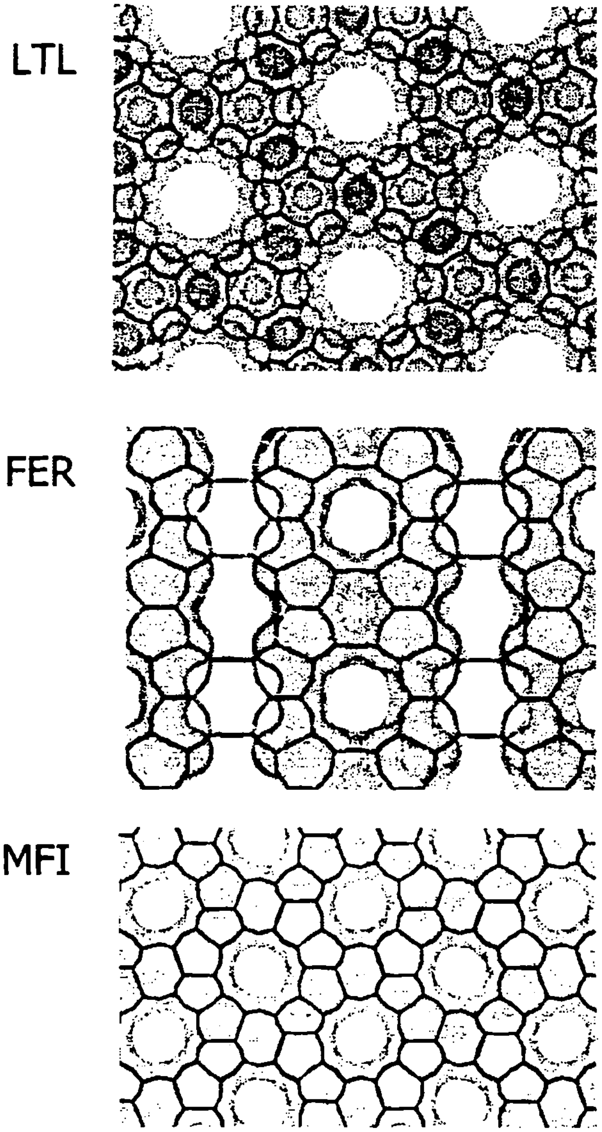

FIGURE 1 The framework topology of three common zeolite structure types: LTL (1D), FER (2D) and MFI (3D)

The term dimensionality refers to channel interconnection, which is relevant to intrazeolite diffusion processes and also to patterned features of zeolite-based nanocomposite materials. Zeolite structures can be viewed[13] as systems consisting of one- two- or three-dimensional channels (1D, 2D or 3D) depending on whether these channels are isolated (1D), or they are mutually intersected either in a plain (2D) or in the three directions of the zeolite framework (3D). Examples are given in Table II, and Fig. 1 depicts some common structure types.

TABLE II Examples of zeotypes showing the three-letter code and details on the pore system

Structure-type code	*Selected isotypes*	*Dimensionality*	*Pore size (Å)*
Small pore			
STI	Stilbite, Stellerite	1D	2.7×5.6
ERI	Eriontie, AlPO-17	3D	3.6×5.1
CHA	Chabazite, AlPO-34	3D	3.8
LTA	Linde A, SAPO-42	3D	4.1
Medium pore			
FER	Ferrierite, ZSM-35	2D	4.2×5.4
AEL	AlPO-11	1D	3.9×6.3
MTT	ZSM-23, EU-13	1D	4.5×5.2
MFI	Silicalite, ZSM-5	3D	5.5
Large pore			
MOR	Mordenite, LZ-211	2D	6.5×7.0
LTL	Perlialite, L	1D	7.1
AFI	AlPO-5, SAPO-5	1D	7.3
FAU	Faujasite, X, Y	3D	7.4
Very large pore			
VFI	VPI-5, MCM-9[a]	1D	12.1
M41S[a]	MCM-41[a]	1D	20 to 80

a. Mobil Corporation codes

Downloaded At: 12:22 15 January 2011

Downloaded At: 12:22 15 January 2011

3. UNDERSTANDING ZEOLITES AND INTRAZEOLITE CHEMISTRY: THE ROLE OF IR SPECTROSCOPY

3.1. Background

Complete understanding of the many (catalytic) chemical processes mediated by zeolites calls for detailed structural characterization at the local (atomic) level. Such a characterization is also much needed in order to extend potential applications of zeolites and zeolite-based materials. Zeolite characterization is a complex task for which many instrumental techniques, as well as computer-based methods, are currently being used. Experimental techniques deserving special mention are classical adsorption studies,[10] X-ray and neutron diffraction,[13–16] high-resolution electron microscopy and electron diffraction,[17–21] NMR spectroscopy[17,22–27] and IR spectroscopy.[28–33]

Diffraction techniques supply precise information concerning periodic structural features of the zeolite framework and the location of extra-framework cations. Neutron diffraction can also be used to probe details about hydrogen bonds and the ordering of tetrahedral atoms in the framework. However, many relevant properties of zeolites stem from non-periodic local arrangements and lattice defects (at the atomic level) which cannot be efficiently characterized by diffraction methods. Synchrotron based techniques (such as EXAFS and XANES) are of some help in this context, but their power is limited by the heterogeneous nature (both in structure and chemical composition) of many local structures in zeolites.[34,35] For instance, the geometry of a zeolite ring (and the resulting local properties) depends on the number of aluminium atoms contained in the ring, which affects the exact extra-framework cation location and related properties. Since zeolites are metastable materials, atom ordering in the framework can be dependent on kinetic factors during zeolite synthesis (instead of being governed by thermodynamics) and this fact limits the power of instrumental techniques which provide averaged values over the whole sample. Similarly, local defects such as extra-framework material and hydroxyl nests[36] (both of which occur very commonly in zeolites) cannot be efficiently characterized by diffraction techniques, X-ray absorption fine structure spectroscopy or even high-resolution electron microscopy.

For a long time, IR spectroscopy has been used as a main technique to characterize zeolites and zeolite-adsorbate systems;[31,33,37,38] the power of this technique will be illustrated in the following sections. It should be pointed out, however, that solid-state NMR spectroscopy is an equally powerful method,[23,24,39,40] particularly after the recent development of 2D multiple-quantum MAS NMR techniques.[41,42] In general, these two spectroscopic methods are more complementary than competitive.

In principle, IR spectroscopy can be directly used to study framework lattice vibrations related to structure type,[43] as well as extra-framework cation vibrations related to cation nature and location.[44] In practice, however, strong coupling among different vibration modes considerably limits the power of this analytical method.[45,46] Much more information can be obtained by using appropriate probe molecules which interact weakly with the zeolite at specific sites. The method is indirect, in the sense that it depends on spectroscopic probes that render the zeolite surface IR-readable. However, by judicious choice of probe molecules a wealth of relevant information can be obtained. Briefly, the vibrational spectra of small molecules, which are dosed from a gas phase, become modified upon interaction with the adsorbing centre (or it is the vibrational pattern of this centre which becomes significantly modified) and the changes observed can often be easily interpreted so that very relevant information is obtained. IR spectroscopy can also be used, in a time-resolved mode, to follow chemical processes taking place within the intra-zeolite space (reaction dynamics). Illustrating examples will now be given.

Downloaded At: 12:22 15 January 2011

3.2. External versus internal surfaces; acid sites and extra-framework species

The catalytically active sites of zeolites are mainly Brønsted acid OH groups, Lewis-acid sites associated with lattice defects or extra-framework material and hetero-atoms (such as Fe, Ga or Ti) which substitute for Al in the aluminosilicate framework. These sites can be located either inside channels or at the external surface of the solid particles. Means for distinguishing internal from external acid sites are needed in order to understand many catalytic processes involving zeolites. For instance, morphoselective (shape-selective) catalysis[47,48] can only be

Downloaded At: 12:22 15 January 2011

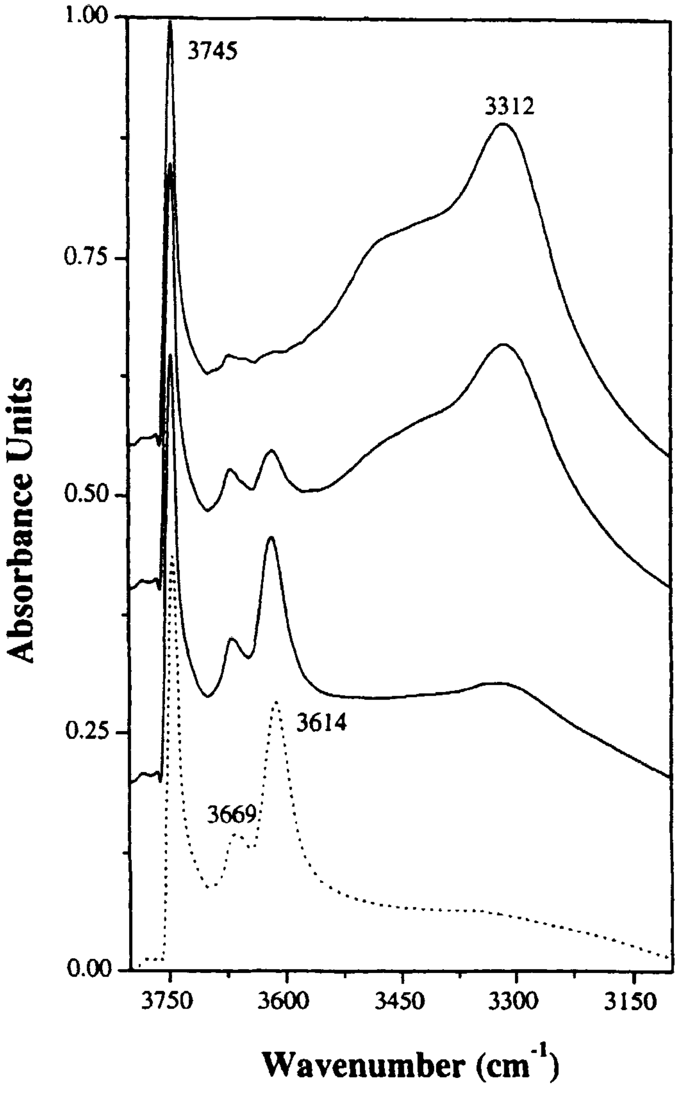

FIGURE 2 Infrared spectra in the O-H stretching region of H-ZSM-5. The dashed line shows the blank spectrum of the zeolite wafer. The remaining spectra were obtained after dosing with CO at 77 K and increasing equilibrium pressure (about 10^{-2} to 10 Torr). For clarity, the spectra are arbitrarily offset on the vertical scale

carried out within internal channels and cages while in other processes, such as the isomerization of substituted xylenes and styrenes, external acidity plays an important role.[49–52]

By choosing two appropriate probe molecules, IR spectroscopy can be used to discriminate between external and internal acid sites. As a case study, let us consider the combined use of CO and $W(CO)_6$ for characterizing the protonic form of ZSM-5. This is an MFI-type zeolite (Table II) which has a 3D channel system with openings of about 0.55 nm in diameter. Carbon monoxide, which has a kinetic diameter of 0.376 nm, finds free access to the intracrystalline space, while $W(CO)_6$ having molecular dimensions of about 0.75 nm[53] can only probe external surfaces.

Fig. 2 shows the IR spectra in the O-H stretching region of a self-supporting wafer of H-ZSM-5, and the effect of increasing doses of CO at 77 K; details about experimental procedures can be found elsewhere.[54] After outgassing at 723 K to remove adsorbed water and other possible contaminants, the zeolite blank spectrum shows two main IR absorption peaks: 3745 and 3614 cm^{-1}, and a weak band at 3669 cm^{-1}. The peak at 3745 cm^{-1} corresponds to silanols while that at 3614 cm^{-1} is the O-H stretching of bridged Si(OH)Al groups[31,54] (Brønsted acid sites) as shown in Scheme I. The weak band at 3669 cm^{-1} can be assigned to hydroxyl groups attached to extra-framework aluminium.[31,55] These extra-framework species, which give rise to Lewis acidity, can be formed in several processes. In the first place incomplete crystallization of the parent gel during zeolite synthesis can leave non-negligible amounts of aluminium hydroxide or hydroxide oxides which after thermal dehydration give rise to coordinatively unsaturated Al^{3+} species (Lewis acid sites). Template burning (zeolites are often synthesized with the help of an organic template agent) can also lead to formation of local defects exposing coordinatively unsaturated Al^{3+} ions.[54]Finally, thermal activation of the zeolite (high-temperature outgassing) very often leads to hydrolysis of Si-O-Al bonds with concomitant formation of extra-framework species and hydroxyl nests[36,54] (another type of local defect).

Adsorption of CO, at 77 K, results in progressive erosion of the band at 3614 cm^{-1} (Fig. 2) and attendant growth of a wider and more intense IR absorption band with a maximum at 3312 cm^{-1}. This is due to formation of the hydrogen-bonded adduct depicted in Scheme I. At the highest CO doses, the band at 3669 cm^{-1} is also eroded while that due to

Downloaded At: 12:22 15 January 2011

Downloaded At: 12:22 15 January 2011

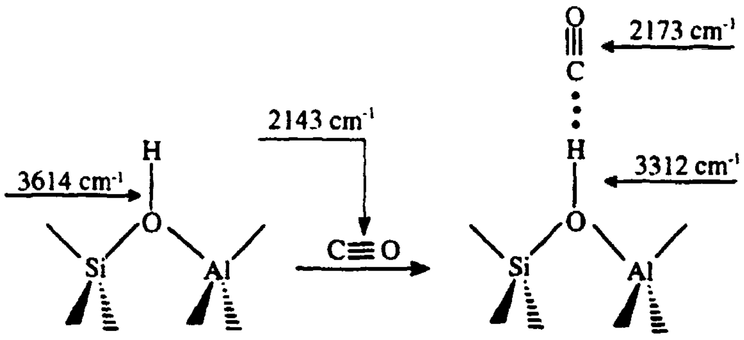

SCHEME I

silanols (3745 cm^{-1}) is only slightly affected. Note, however, that discrimination between acid sites located inside channels or at external surfaces is not possible at this stage, since CO has direct access to both of them.

Fig. 3 shows the IR spectra, in the O-H stretching region, of H-ZSM-5 with increasing doses of adsorbed $W(CO)_6$. Metal carbonyls are known[56] to interact with hydroxy groups of (hydroxylated) metal oxides and zeolites leading to adduct formation as shown in Scheme II. Such a hydrogen-bonding interaction leads to perturbation of the corresponding O-H stretching modes in a similar way as already described for OH···CO adducts. Fig. 3 shows that (*i*) the IR absorption band at 3669 cm^{-1} is not affected by adsorption of the metal carbonyl. (*ii*) The band at 3614 cm^{-1}, corresponding to Brønsted acid sites, is only slightly (but significantly) eroded; see inset in Fig. 3. (*iii*) The silanol band at 3745 cm^{-1} is significantly eroded, but much of it remains even after saturation with $W(CO)_6$.

Since CO has free access to the zeolite channels while the diameter of the $W(CO)_6$molecule is greater than the channel free entrance dimension, comparison between IR spectra in Figs. 2 and 3 demonstrates the following points. (*i*) The species giving rise to the O-H stretching band at 3669 cm^{-1} are occluded inside the zeolite channels; note that they were probed by CO but not so by $W(CO)_6$. (*ii*) Silanols are located both

Downloaded At: 12:22 15 January 2011

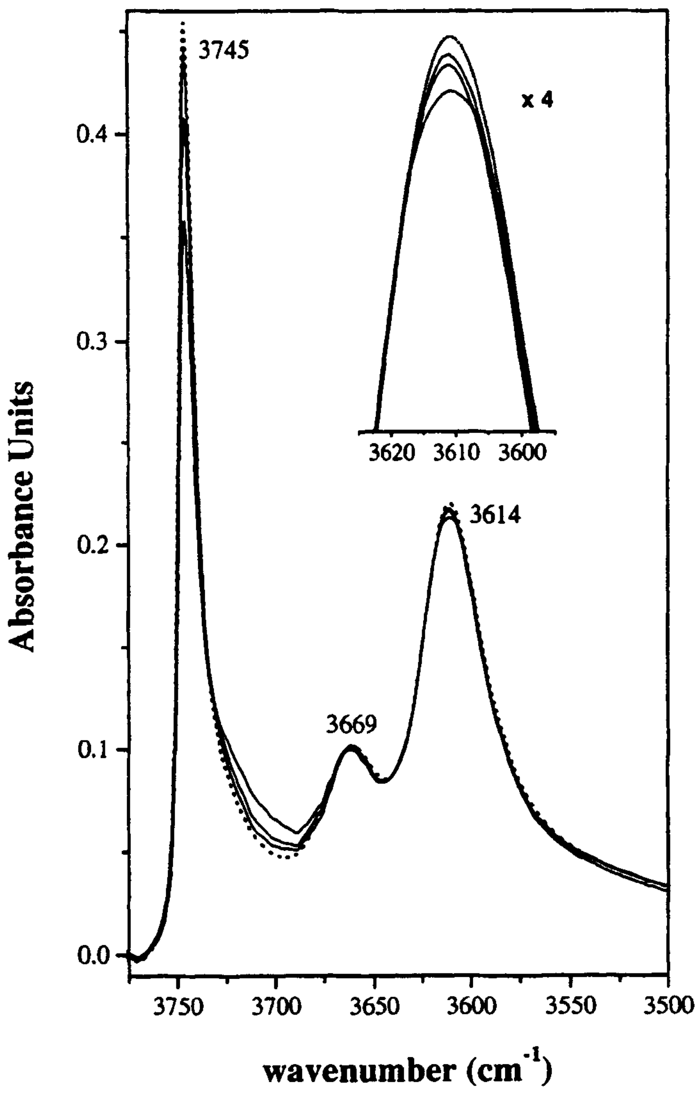

FIGURE 3 Effect of dosing with $W(CO)_6$ on the IR spectrum of H-ZSM-5. The zeolite blank spectrum (dashed line) is increasingly eroded upon adsorption of the metal carbonyl; but much remains ever after saturation. The inset shows an expanded view of the peak at 3614 cm^{-1}

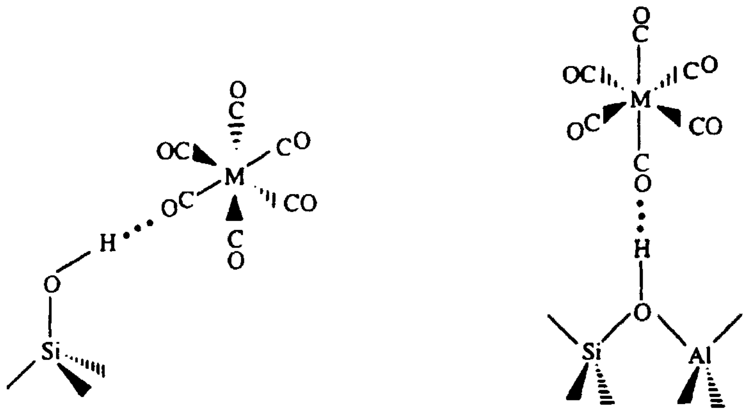

SCHEME II

at external surfaces (affected by adsorbed $W(CO)_6$) and inside zeolite channels (not accessible to the metal carbonyl). (*iii*) Bridging O-H groups (Brønsted-acid sites) are mainly internal, but a small fraction of these sites is located at the external surface of the zeolite crystals. This is relevant to several catalysed processes where external acid sites can have an important role, as already mentioned.

The foregoing example shows how IR spectroscopy can be used to differentiate external from internal features of zeolites and related microporous materials. The selection of probe molecules for accomplishing such a task is not unique. For instance, the couple formed by acetonitrile and adamantane-carbonitrile can equally well be used[57,58] for IR spectroscopic studies and, in a similar fashion, perfluorotributylamine (a weakly basic molecule having a diameter of 0.94 nm) was recently used[59] for quantitative determination of external acidity by MAS NMR. It is relevant to add that, even for the same structure type and (average) chemical composition, the percentage of acid sites appearing at the external surface of a zeolite can be critically dependent on such factors as crystallite size, synthesis conditions and post-synthesis thermal treatments; therefore, characterization is usually needed for every particular batch being used.

The C-O stretching region of the spectra shown in Fig. 2 is depicted in Fig. 4. Briefly, CO adsorbed (at 77 K) on H-ZSM-5 shows a main IR

Downloaded At: 12:22 15 January 2011

Downloaded At: 12:22 15 January 2011

absorption band at 2173 cm^{-1} which corresponds to the C-O stretching of hydrogen-bonded CO (Scheme I). A weaker, and complex, band appears in the 2210–2240 cm^{-1} range with a maximum at 2228 cm^{-1} and a shoulder at 2221 cm^{-1}(see inset in Fig. 4). This band, which saturates at low CO doses, corresponds to the C-O stretching of $Al^{3+}\cdots CO$ adducts formed on dehydroxylated (Al_2O_3) extra-framework species.[31,54] The complex nature of the band reveals the presence of different types of coordinatively unsaturated Al^{3+} ions having different Lewis-acid strength. Such Lewis acid centres are also relevant to catalytic processes, and they can be further characterized by using other probe molecules. For instance, dinitrogen can be superior to CO for studying details of cation unsaturated coordination.[60] Absence of a dipole moment in the non-polarized N_2molecule avoids complications due to signals coming from the gas phase (which, for CO, can be seen at about 2138 cm^{-1} in Fig. 4). When polarized by the electric field created by surface-exposed cations, N_2 becomes IR-active and the intensity of the field-induced IR absorption is proportional to the second power of the electric field. This fact renders dinitrogen a very sensitive molecule for probing cations having different degrees of coordinative unsaturation, which leads to different values of the corresponding (net) electric field.[60]

To conclude this section, it is worth mentioning that basic sites in zeolites (*e.g.* framework oxygens) can be studied by using weakly acid molecules (such as CO_2, SO_2 or $CHCl_3$) as IR spectroscopic probes.[30,33,61,62] Other molecules, such as dihydrogen, have the potential to interact simultaneously with both ions in a cation-anion pair[63] (as shown by *ab initio* quantum chemical calculations) and hence they can be used as IR spectroscopic probes for dual acid-base sites,[31,64] rather than only for cation or anion centres.

3.3. Intrazeolite electric fields

Molecules entering zeolite channels and cages are exposed to strong electric fields generated by extra-framework cations (and nearby framework anions). These electric fields can significantly alter the electron distribution of adsorbed molecules, and hence their reactivity patterns.

Downloaded At: 12:22 15 January 2011

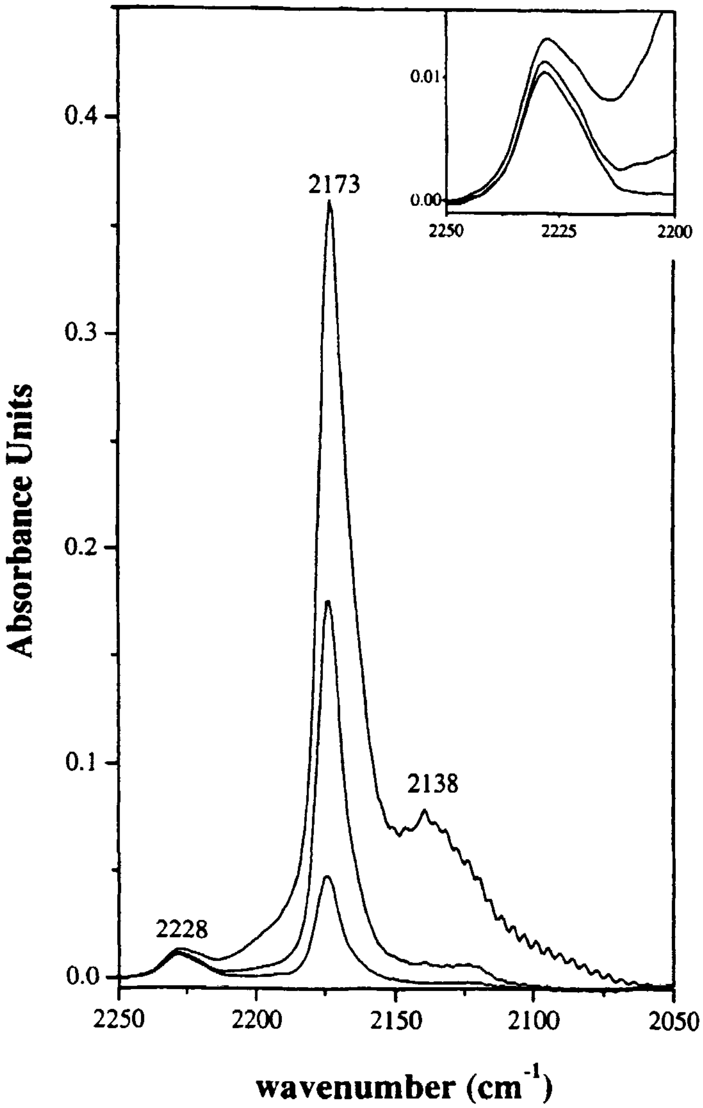

FIGURE 4 C-O stretching region of the same spectra shown in Fig. 2. The zeolite blank spectrum has been subtracted. Inset shows magnification of the band at 2228 cm^{-1}

Therefore, quantification of electric field strength can help to understand intrazeolite chemistry.

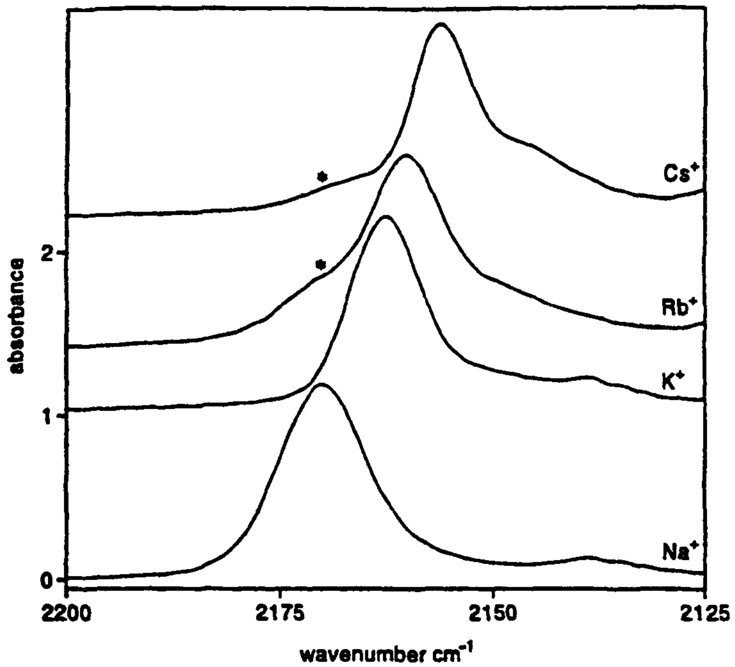

FIGURE 5 Infrared spectra of CO adsorbed at 77 K on M^+-ZSM-5 (M= Na, K, Rb, Cs). The downwards shift of the peak maximum from Na^+ to Cs^+ is clearly seen. The shoulder marked with an asterisk corresponds to a small fraction of Na^+ still present after ion exchange (ref. 31)

Suitable probe molecules can be used for IR monitoring of charge-balancing cations and their associated electric fields; a good example of such a probe molecule is carbon monoxide. IR spectra of CO adsorbed, at liquid nitrogen temperature, on M^+-ZSM-5 (M= Na, K, Rb, Cs) are depicted in Fig. 5. They all show a main IR absorption band which is upward shifted with respect to free CO: 2143 cm^{-1}. This cation-specific band corresponds to the fundamental C-O stretching mode of carbon monoxide interacting through the carbon atom with the corresponding

Downloaded At: 12:22 15 January 2011

metal ion. The hypsochromic frequency shift, Δυ, arises (mainly) from the vibrational Stark effect of the dipolar molecule (CO has a permanent dipole moment, μ= 0.112 D) under the influence of the axial electric field, E, created by the cation in $M^+\cdots CO$ adducts. Neglecting second order (quadratic) terms, the magnitude of Δυ is given by: $\Delta\upsilon = k_{ST}E$, where k_{ST} is the vibrational Stark constant for CO, which has the value[65] k_{ST}= 4.29×10^{-9} m cm^{-1} V^{-1}. To a first approximation, the above expression can be used to calculate the value of the electric field from IR spectra of adsorbed CO; more refined quantum chemical treatments are also available.[66]

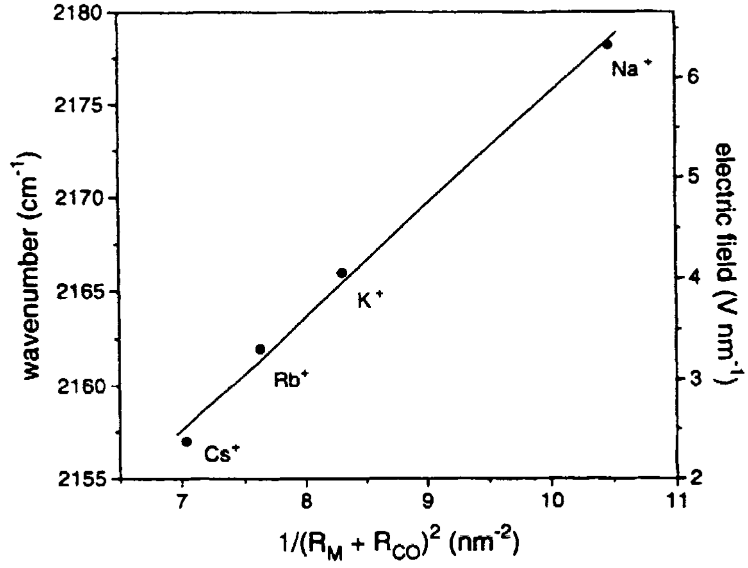

FIGURE 6 C-O stretching frequency, and corresponding electric field, versus $1/(R_M+R_{CO})^2$ for alkali-metal-exchanged ZSM-5 zeolites

Fig. 6 shows that, as expected from the foregoing considerations, a linear correlation exists between the C-O stretching frequency and the corresponding value of $1/(R_M+R_{CO})^2$, where R_M is the cation radius and R_{CO}= 0.21 nm. Values of intrazeolite electric fields deduced from IR spectroscopy of adsorbed CO are given in Table III. Other probe

Downloaded At: 12:22 15 January 2011

molecules can equally well be used for the same purpose. Thus, Cohen de Lara *et al.*,[67] and Böse and Förster[68]determined the electric field in zeolites Na-A, NaCa-A and Ca-A from the integrated IR intensities of adsorbed dinitrogen; their results are consistent with those shown in Table III. Finally, it should be noted that, for the same cation, the magnitude of the net positive electric field varies slightly for different zeolites. This is due to a variable framework topology which affects the geometrical arrangement and number of nearby (framework) anions, and hence the net field at the cation site. Detailed knowledge of intrazeolite electric fields is needed for understanding the role of differently located extra-framework cations and their effective charges. This applies not only to catalytic activity but also to other practical applications of zeolites, such as gas-separation processes and the formation (and properties) of intrazeolite nanostructures in guest-host composite materials.

Downloaded At: 12:22 15 January 2011

TABLE III Internal electric field in some selected zeolites

Zeolite (cationic form)	*Electric field (V nm^{-1})*
Na-ZSM-5	6.3
K-ZSM-5	4.1
Rb-ZSM-5	3.4
Cs-ZSM-5	2.4
Na-MOR	6.1
Na-Y	5.2
Ca-Y	10.2
Mg-ETS-10[a]	11.5

[a] ETS-10 is a titanosilicate molecular sieve having a structure-type analogous to that of zeolite β.

3.4. Following up intrazeolite processes

Infrared spectroscopy has proved to be a powerful method for monitoring the reaction dynamics of intrazeolite chemical processes. In time-resolved experiments short-lived intermediates involved in transformations of adsorbed molecules can be monitored and valuable information concerning reaction mechanisms can thus be gathered. Detection of transient reaction intermediates is often facilitated by the rather high energy resolution of IR spectroscopy which enables the measurement of small frequency shifts, and also band shape analysis, to be performed.

There have been many studies of intrazeolite processes by means of IR spectroscopy. Zecchina *et al.*[69] used time-resolved (sub-second) FTIR spectroscopy to follow the sequence of events leading to ethene and propene oligomerization inside the channels of H-ZSM-5. They showed how oligomerization is preceeded by formation of a hydrogen-bonded π-complex followed by olefin protonation, which resulted to be the slowest process in the reaction chain. Formation of the hydrogen-bonded complex was clearly monitored by the corresponding downward shift of the characteristic stretching mode of both the zeolite Si(OH)Al Brønsted acid group and the alkene double bond, as shown (for ethene) in Scheme III. Similar studies were conducted[70] on the oligomerization of acetylene (and substituted acetylenes) on H-ZSM-5, which leads to formation of intrazeolite conjugated polymers; also in this case protonation of the hydrogen-bonded complex was found to be the slow process.

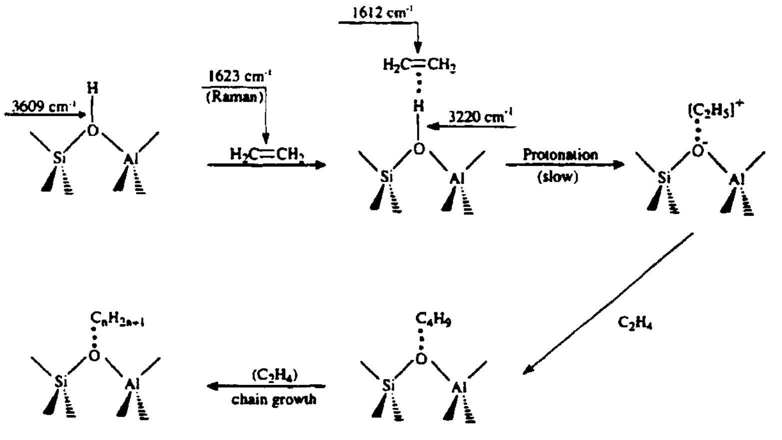

SCHEME III

Bonn *et al.*[71] have demonstrated the use of laser assisted picosecond IR spectroscopy in a study of the vibrational dynamics of methanol clus-

Downloaded At: 12:22 15 January 2011

ters in the zeolite Na-Y. Comparison with the behaviour of similar clusters in solution (carbon tetrachloride) showed that in both systems excitation with resonant infrared pulses leads to cleavage of hydrogen bonds and cluster fragmentation. However, both the predissociation and the reassociation time were found to be markedly larger for methanol clusters in the zeolite. Step-scan FTIR spectroscopy on the microsecond time scale was used[72] to detect formation of a transient acetyl radical during photochemically induced Fries rearrangement of 1-naphthyl acetate encaged in Na-Y. These examples show the potential of time-resolved IR spectroscopy for mechanistic studies of chemical reactions within microporous solids. In particular, photochemical studies begin to open up many possibilities for clever design of dye-zeolite materials for light energy harvesting in solar cells,[73,74] and also for the fabrication of miniaturized dye lasers.

Downloaded At: 12:22 15 January 2011

3.5. Lessons from variable-temperature IR spectroscopy

Understanding chemistry inside zeolites, and the use of these materials as nano-reactors, calls for a careful study of all the possible interactions of adsorbed molecules with the host material. Infrared spectra of adsorbed molecules often contain more details than what is possible to analyse in the standard use of this technique, but means can be devised to extract valuable information from such details. This section highlights the potential of variable-temperature IR spectroscopy.

As an example, we shall consider the case of CO adsorbed on zeolites of the MFI and FAU structural types. As already stated in section 3.3, the IR spectra of CO adsorbed on zeolites show a main band corresponding to the fundamental C-O stretching mode of $M^{+}\cdots CO$ adducts, where M is the extra-framework cation present in the zeolite (Fig. 5). However, this high-frequency (HF) band is almost invariably accompanied by a minor low-frequency (LF) band downward shifted with respect to free CO, as shown in Fig. 7. Quantum chemical calculations[75] proved that this LF band corresponds to the C-O stretching of $M^{+}\cdots OC$ adducts where carbon monoxide interacts with the metal cation through the oxygen atom. In principle, C-bonded and O-bonded adducts could either be formed on different cation sites, or they could be the result of an isomerization equilibrium at the same site; a case of linkage isomerism. Variable temperature FTIR spectroscopy has resolved this dichotomy.

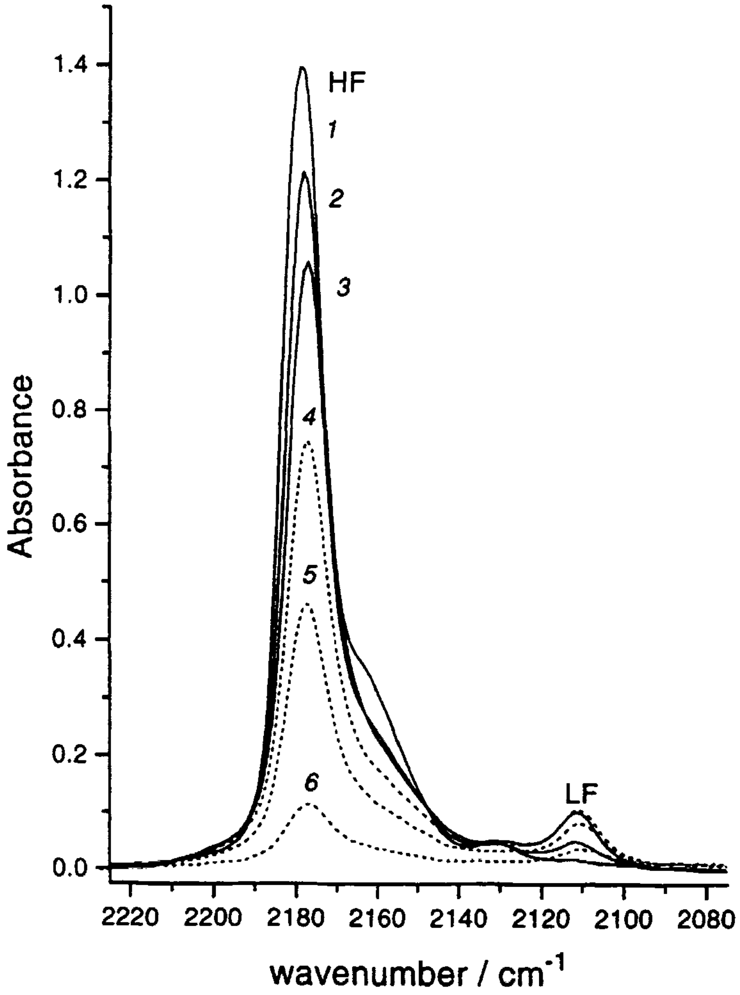

FIGURE 7 Variable-temperature FTIR spectra of CO (ca. 0.8 Torr) adsorbed on Na-ZSM-5: *1*, 83; *2*, 153; *3*, 203; *4*, 233; *5*, 253; *6*, 293 K. Note that the HF band steadily decreases as temperature is raised, whereas the LF band first increases (spectra *1* to *3*) and then decreases (*4* to *6*)

Downloaded At: 12:22 15 January 2011

Downloaded At: 12:22 15 January 2011

Fig. 7 shows some selected variable temperature spectra[76] for CO adsorbed on Na^+-ZSM-5 (an MFI type zeolite). Correlation between the HF and LF bands is clearly seen. When temperature is increased from 83 to 203 K the intensity of the HF band (A_{HF}) decreases, whereas that of the LF band (A_{LF}) increases. At higher temperatures both bands decrease (because the net amount of adsorbed CO decreases) but the ratio of integrated intensities A_{LF}/A_{HF} increases over the whole temperature range. This is precisely the behaviour to be expected for an isomerization equilibrium (involving the same cation site) of the type:

$$\text{-Na}^+ \cdots \text{CO} \longrightarrow \text{Z-Na}^+ \cdots \text{OC}$$

Where Z stands for the zeolite framework.

The intensity ratio A_{LF}/A_{HF} should be proportional to the equilibrium constant, *k*, of the above process through the corresponding ratio of molar absorption coefficients, $\varepsilon_{LF}/\varepsilon_{HF}$. That is, $k = (A_{LF}/A_{HF})(\varepsilon_{HF}/\varepsilon_{LF})$ The temperature dependence of *k* was found to conform to the van't Hoff relationship: $\ln k = -\Delta H^o/RT + \Delta S^o/R$ This is shown in Fig. 8, where data from spectra taken at many different temperature values[76] are represented. The observed linear plot of $\ln(A_{LF}/A_{HF})$ versus $1/T$ provides clear evidence that $Z\text{-}Na^+\cdots CO$ and $Z\text{-}Na^+\cdots OC$ species are in a temperature dependent equilibrium. Note that constant values of ΔH^o and ΔS^o (a condition required for correct application of the van't Hoff relationship) imply that $\Delta C_p = 0$. Computational results for the above isomerization equilibrium between C-bonded and O-bonded species have shown that the corresponding ΔC_pvalue is, in fact, negligible.[75] When studied by means of variable temperature FTIR spectroscopy,[77] CO adsorbed on Na^+-Y (a zeolite of the FAU structure type) gave also a linear plot of $\ln(A_{LF}/A_{HF})$ versus $1/T$. However, corresponding values of ΔH^o (the enthalpy term for the isomerization process described above) were found to be significantly different: $\Delta H^o = 3.8$ kJ mol^{-1} for the CO/Na^+-ZSM-5 system, and $\Delta H^o = 2.4$ kJ mol^{-1} for CO/Na^+-Y. This difference neatly reflects the influence of the zeolite framework.

Finally, it should be noted that other heteroatomic molecules could show a similar amphipathic behaviour as that shown by CO. Indeed, there is some evidence that nitric oxide can interact with extra-framework cations in zeolites forming N-bonded and O-bonded adducts.[78] Different orientations of adsorbed molecules in the intrazeolite electric fields should lead to significant variations in their electron distribution and (presumably) reactivity patterns. This is a field deserving further investigation; there is much to learn and much to do.

4. RECENT DEVELOPMENTS

Zeolite materials science is a very active research field. A comprehensive account of recent developments in this field is outside the scope of this article, but a few examples will suffice to illustrate promising developments.

Many metallic and semiconductor clusters have been synthesized within the cavities of zeolites: alkali metal clusters, silver, bismuth, selenium, silicon, CdS, GaAs, and many others. Procedures for preparing zeolite-confined nanoclusters include dosing from a gas or liquid phase, ion exchange, co-condensation with framework precursors and solid-state reaction. As a result of quantum size effects, these nanoclusters exhibit novel (and sometimes unexpected) properties.[79] For instance, it has been reported[80] that silicon nanoclusters (about 12 atoms in size) in zeolite-Y show strong photoluminescence at room temperature and have a direct band gap, with E_g= 2.2 eV. By contrast, bulk silicon is an indirect band gap semiconductor having Eg= 1.1 eV. So that, not only the magnitude of Eg can be engineered but also the band structure can be efficiently modified by using zeolites as host materials for semiconductors.

Polymerization of organic monomers inside zeolite channels provides a means to obtain single chains of conjugated polymers isolated in a dielectric matrix.[8,9,70] It is possible to functionalize these polymers with various prosthetic groups. By changing the nature of these groups, specific interaction with external agents can be developed so as to engineer molecular devices such as sensors, transducers and optical memories. Conducting (single chain) wires and electroluminescent chromophores (depending on how the polymer is doped) can also be obtained. The fact that the polymer array is periodic, because of the inherent periodicity of the zeolite host material, bears hopes that individual elements could perhaps be addressed. While this is (admittedly) a perspective for the future, the possibility of gaining insights into long standing questions in molecular electronics, such as single chain conductivity, belongs already into the present. A related field concerns encapsulation of organic dye molecules in molecular sieves,[81] which leads to composite

Downloaded At: 12:22 15 January 2011

Downloaded At: 12:22 15 January 2011

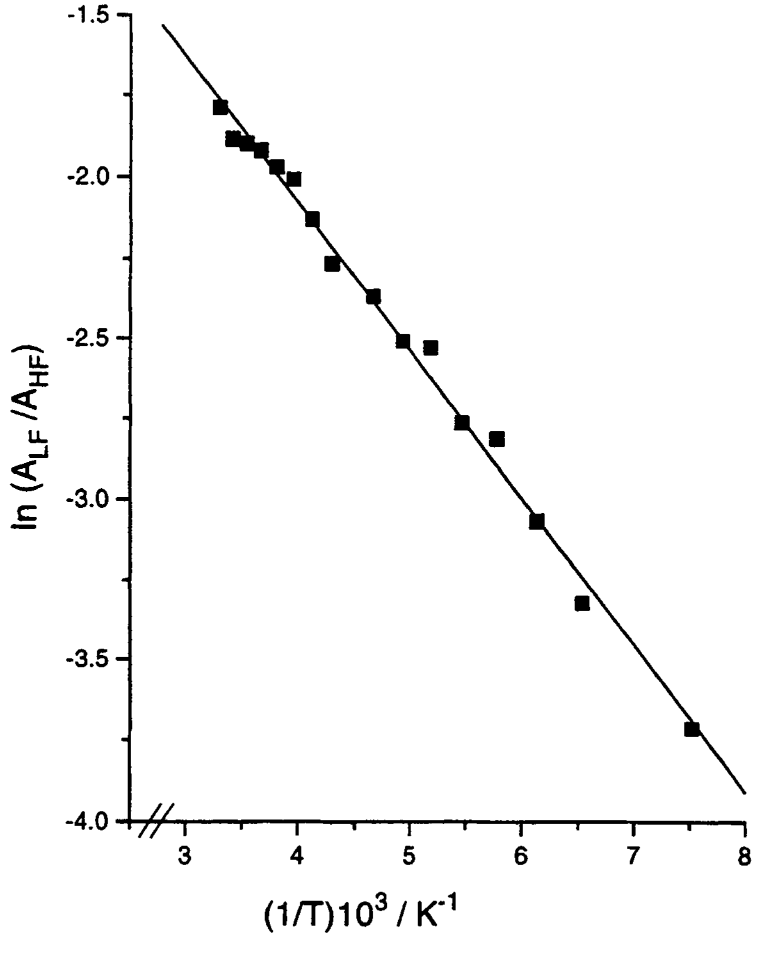

FIGURE 8 The van't Hoff plot of the natural logarithm of the intensity ratio of LF and HF bands versus the reciprocal of the temperature (c.f. Fig. 7 and ref. 76)

materials having potential applications as pigments, or in gas sensing, frequency doubling and microlasing. Nanostructures having optical wavelength scale have considerable interest in quantum optics and device technology. Note that light generation efficiency can be expected to increase in wavelength-scale microlasers, since the spontaneous emission rate can be conveniently modified by reduction of at least one lateral dimension to the order of magnitude of one wavelength.

Concerning applications in catalytic and other chemical processes (such as removal of toxic metals or affinity chromatography) there have recently been significant advances in the preparation of functionalized zeolites and other molecular sieves. In general, functionalization involves reaction of zeolite silanols with organic molecules containing *e.g.* phenyl, amino or thiol groups. Procedures include template-directed co-condensation with zeolite precursors, ion exchange reactions and sol-gel methods involving metal alkoxides. Several types of mesoporous organic-inorganic hybrid materials have thus been prepared, and their potential applications are currently being explored.[82–84] Zeolites can also be turned into constrained chiral catalysts by grafting optically active moieties inside their channels and cavities.[85,86] For some processes, space confinement results in amplification of the effect of the grafted chiral centre, which leads to unprecedented enantiomeric and diastereomeric excess in the reaction products.[86]

Regarding IR spectroscopic studies, recent developments include the use of far IR synchrotron radiation. Synchrotron sources make available very intense IR radiation which can be used to explore the spectral region where zeolite wafers are scarcely transparent. An example is a recent study[87] of the metal-carbon vibration (υ_{MC}) of CO adsorbed on zeolites. Fig. 9 shows the IR spectrum of CO adsorbed on the zeolite Na-Y. Besides the already discussed bands at 2171 and at 2122 cm^{-1}(which correspond, respectively, to the C-O stretching of $Na^+\cdots CO$ and $Na^+\cdots OC$ adducts) a very weak band is observed at 2310 cm^{-1}. This weak band was thought to correspond to the combination mode $\upsilon_{CO}+\upsilon_{MC}$ of $Na^+\cdots CO$ adducts, but direct observation of the υ_{MC} mode was not possible in the standard use of IR spectroscopy. However, the spectrum taken by using synchrotron radiation[87] clearly shows the metal-carbon vibration mode at 139 cm^{-1} (inset in Fig. 9) thus confirming assignment of the combination mode. Fig. 10 shows a plot of υ_{MC} versus the inverse of the cation radius (r) for alkali-metal-exchanged ZSM-5 zeolites; the parameter 1/r is used as a measure of the cation polarizing power. A linear correlation is obtained, as expected. It should be noted that the frequency of the cation-carbon stretching vibration is very sensitive to the specific cation present in the zeolite, and detection of this mode gives precise structural information. It also provides a very sensitive estimation of the strength of the cation-CO interaction.

Downloaded At: 12:22 15 January 2011

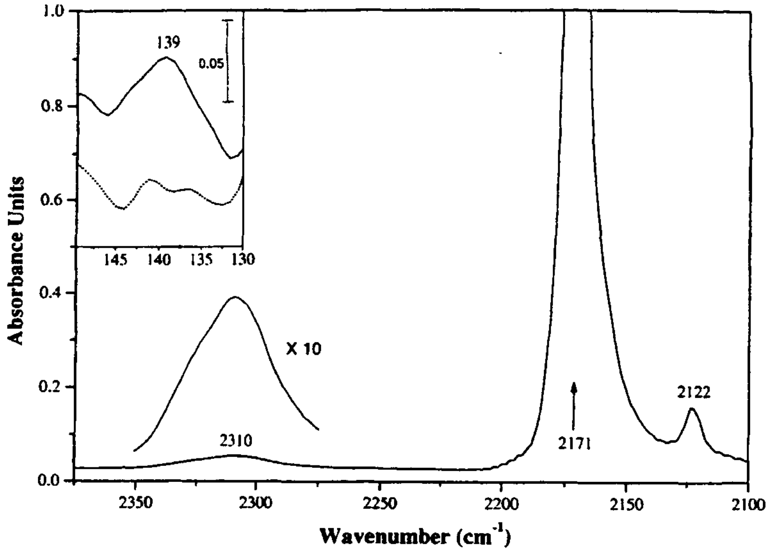

FIGURE 9 Infrared spectrum of CO adsorbed at 77 K on the zeolite Na-Y, at an equilibrium pressure of about 5 Torr. Inset shows the far IR region obtained by using synchrotron radiation; the dashed line is the zeolite blank spectrum, the full line is the spectrum of the zeolite containing adsorbed CO (ref. 87)

SUMMARY AND OUTLOOK

Zeolites and related periodic microporous materials have already proved to have outstanding properties relevant to applications in many technological fields such as molecular sieving, ion exchange or shape-selective catalysis, to name only a few examples. It is becoming increasingly clear that many other developments are possible. Versatility in topology and chemical composition opens up the opportunity for engineering the intracrystalline space of zeolites to suit the needs of a large variety of technical applications.

By choosing the right topology, framework composition and extra-framework cation a fine control can be achieved on the size and shape of the intracrystalline space, as well as on the geometry and strength of intrazeolite electric fields. This should lead to an attendant control on the way in which adsorbed molecules can be activated and

Downloaded At: 12:22 15 January 2011

Downloaded At: 12:22 15 January 2011

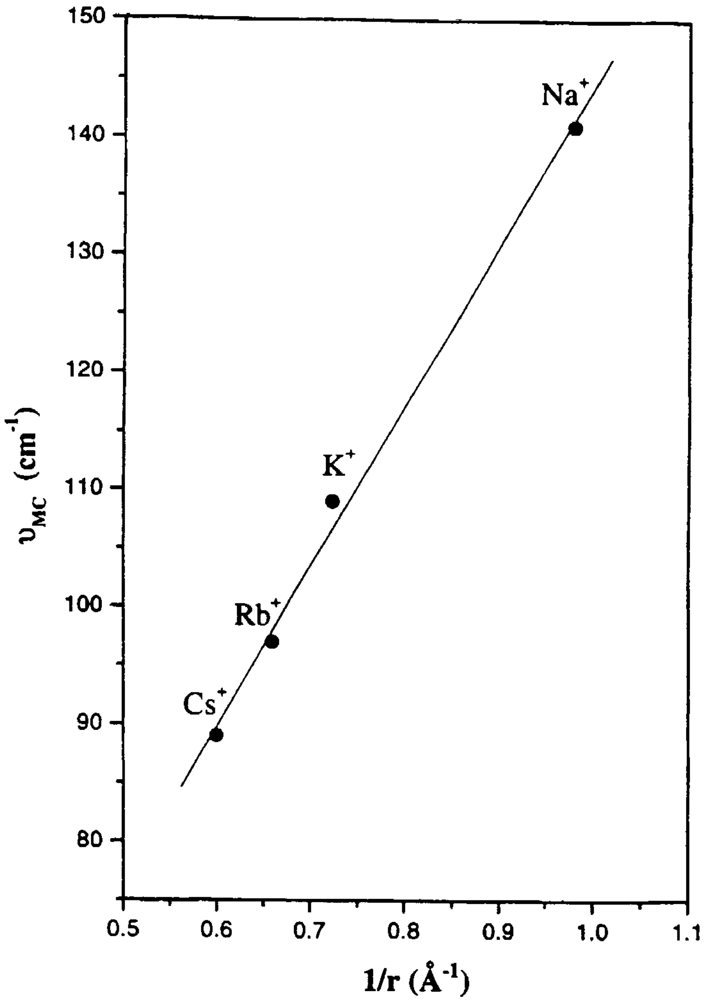

FIGURE 10 Plot of the wavenumber of the cation-carbon stretching vibration versus the inverse of the cation radius for CO adsorbed on alkali-metal-exchanged ZSM-5 zeolites

their reactivity patterns modified. By using zeolites as nano-reactors, a new strategy is emerging for controlling chemical processes. The classical way to modify reactivity of a molecule is to put substituents in it;

organic chemists have been successfully exploiting this method for a long time. Now the molecule can be kept as it is, and the surroundings changed, and space controls reactivity.

Incorporation of functional groups and chiral centres in zeolites, either by grafting or by tucking them into the zeolite framework, represents a further step along the same road. Chiral chambers can thus be created which act as very selective catalysts for the asymmetric synthesis of fine chemicals.

Zeolites are also being used as crystalline host materials for encapsulating and organizing dye molecules, semiconductor clusters and supramolecular entities inside their pores. Space confinement and host-guest (electrostatic) interaction results in nanocomposite materials possessing novel optical, electronic and magnetic properties. Potential technological applications can be expected in a number of fields, such as chemical and biological sensing, semiconductor devices and photonics. The unique opportunity which zeolites offer for preparing three-dimensional arrays of mutually interacting clusters having a well-defined geometry can also be exploited for fundamental studies. For instance, the optical properties or semiconductor nanocrystals (quantum dots) are well understood, but little is known about nanocrystalline networks having long range order. Zeolites allow these networks to be prepared and studied.

Progress in most of the above fields depends quite critically on an increased ability to synthesize high-quality zeolite crystals and to characterize zeolites and zeolite-based materials at the local (atomic) level. At present, imperfections do exist in these materials which often affect relevant properties in an uncontrolled manner, and this constitutes a setback for further developments. It should be clear that better characterization methods would help to design improved synthesis procedures.

For zeolite characterization, many instrumental techniques (most of them spectroscopic) are currently being applied, and indeed concurrent use of several techniques is highly desirable. Much can also be learnt from the interplay between experimental research and computer assisted calculations and modelling. The use of infrared spectroscopy for zeolite characterization was highlighted in this article, including modes based on molecular probes, variable temperature measurements and infrared radiation from synchrotron sources. It was also shown how time-domain IR spectroscopy can be used for detecting transient species and studying intrazeolite chemical processes. Increasing use[88–90] of ultrafast IR spec-

Downloaded At: 12:22 15 January 2011

troscopy facilities and variable temperature equipment should boost the already strong contribution of this technique to the study of zeolites and intrazeolite chemistry. Expectations also exist on the use of very low temperature (liquid helium) infrared spectroscopy for zeolite characterization, which would give the opportunity to gain knowledge about some long standing questions, such as the fine structure of hydroxy groups in zeolites and related microporous materials.

Propelled by its many foreseeable applications, the field of microporous material science has gathered considerable momentum in recent years, which led to improved methods of both synthesis and characterization of zeolites and zeolite-based materials. However, given the many questions that still remain open, and the vast possibilities for further development, this field should remain exciting for years to come. There seems to be ample room for imaginative thinking and for creative research.

Downloaded At: 12:22 15 January 2011

Acknowledgements

The author thanks Dr. S. Bordiga (Università di Torino) and Drs. M. Peñarroya Mentruit and G. Turnes Palomino (Universidad de las Islas Baleares) for help with computer graphics.

References

1. W. M. Meier and D. H. Olson, Atlas of Zeolite Structure Types, Butterworth-Heinemann, London 1992.
2. C. T. Kresge, M. E. Leonowicz, W. J. Roth, J. C. Bartuli and J. S. Beck, Nature, **359**, 710 (1992).
3. G. D. Stucky, Curr. Opin. Solid State Mater. Sci. **3**, 11, (1998).
4. C. Cascales, E. Gutiérrez-Puebla, M. Iglesias, M. A. Monge and C. Ruíz-Valero, Angew. Chem. Int. Ed. **38**, 2436 (1999).
5. A. K. Cheetham, G. Férey and T. Loiseau, Angew. Chem. Int. Ed. **38**, 3268 (1999).
6. P. B. Venuto, Microporous Mater. **2**, 297 (1994).
7. G. A. Ozin, A. Kuperman and A. Stein, Angew. Chem. Int. Ed. **28**, 359 (1989).
8. G. D. Stucky, Progr. Inorg. Chem. **40**, 99 (1992).
9. K. Moller and T. Bein, Chem. Mater. **10**, 2950 (1998).
10. D. W. Breck, Zeolite Molecular Sieves, Wiley, New York, 1974.
11. R. M. Barrer, Zeolites and Clay Minerals as Sorbents and Molecular Sieves, Academic Press, London, 1978.
12. R. M. Barrer, Hydrothermal Chemistry of Zeolites, Academic Press, New York, 1982.
13. R. Szostak, Molecular Sieves, Van Nostrand Reinhold, New York, 1989.
14. L. B. McCusker, Acta Cryst. **A47**, 297 (1991).
15. M. Czjek, H. Jobic, A. N. Fitch and T. Vogt, J. Phys. Chem. **96**, 1535 (1992).

52. S. Melson and F. Schüth, J. Catal. **170**, 46 (1997).
53. S.P. Arnesen and H. M. Seip, Acta Chem. Scand. **20**, 2711 (1966).
54. C. Otero Areán, G. Turnes Palomino, E. Escalona Platero and M. Peñarroya Mentruit, J. Chem. Soc. Dalton Trans. 873 (1997).
55. G. L. Woolery, L. B. Alemany, R. M. Dessau and A. W. Chester, Zeolites **6**, 14 (1986).
56. A. Zecchina and C. Otero Areán, Catal. Rev. Sci. Eng. **35**, 261 (1993).
57. C. Otero Areán, E. Escalona Platero, M. Peñarroya Mentruit, M. Rodríguez Delgado, F. X. Llabrés i Xamena, A. García-Raso and C. Morterra, Microporous Mesoporous Mater. **34**, 55 (2000).
58. C. Otero Areán, M. Rodríguez Delgado, M. Peñarroya Mentruit, F. X. Llabrés i Xamena and C. Morterra, Stud. Surf. Sci. Catal., **130**, 3137 (2000).
59. W. Zhang, D. Ma, X. Liu, X. Liu and X. Bao, Chem. Commun. 1091 (1999).
60. C. Otero Areán, G. Turnes Palomino, F. Geobaldo and A. Zecchina, J. Phys. Chem. **100**, 6678 (1996).
61. P. A. Jacobs, F. M. Van Cauwelaert and E. F. Vansant, J. Chem. Soc. Faraday Trans. 1, **69**, 2130 (1973).
62. H. G. Karge, M. Laniecki and M. Ziolek, J. Catal. **109**, 252 (1988).
63. I. N. Senchenya and V. B. Kazansky, Kinet. Katal. **29**, 1131 (1988).
64. S. Bordiga, E. Garrone, C. Lamberti, A. Zecchina, C. Otero Areán, V. B. Kazansky and L. M. Kustov, J. Chem. Soc. Faraday Trans. **90**, 3367 (1994).
65. D. K. Lambert, Solid State Commun. **51**, 297 (1984).
66. G. Pacchioni, G. Cogliandro and P. S. Bagus, Int. J. Quant. Chem. **42**, 1115 (1992).
67. B. Barrachin and E. Cohen de Lara, J. Chem. Soc. Faraday Trans. 2, **82**, 1953 (1986).
68. H. Böse and H. Förster, J. Mol. Struct. **218**, 393 (1990).
69. G. Spoto, S. Bordiga, G. Ricchiardi, D. Scarano, A. Zecchina and E. Borello, J. Chem. Soc. Faraday Trans. **90**, 2827 (1994).
70. S. Bordiga, G. Ricchiardi, G. Spoto, D. Scarano, L. Carnelli, A. Zecchina and C. Otero Areán, J. Chem. Soc. Faraday Trans. **89**, 1843 (1993).
71. M. Bonn, H. J. Bakker, A. W. Kleyn and R. A. van Santen, J. Phys. Chem. **100**, 15301 (1996).
72. S. Vasenkov and H. Frei, J. Am. Chem. Soc. **120**, 4031 (1998).
73. F. Binder, G. Calzaferri and N. Gfeller, Sol. Energy Mater. Sol. Cells **38**, 175 (1995).
74. B. Hennessy, S. Megelski, C. Marcolli, V. Shklover, C. Bärlocher and G. Calzaferri, J. Phys. Chem. B **103**, 3340 (1999).
75. P. Ugliengo, E. Garrone, A. M. Ferrari, A. Zecchina and C. Otero Areán, J. Phys. Chem. B **103**, 4839 (1999).
76. C. Otero Areán, A. A. Tsyganenko, E. Escalona Platero, E. Garrone and A. Zecchina, Angew. Chem. Int. Ed. **37**, 3161 (1998).
77. A. A. Tsyganenko, E. Escalona Platero, C. Otero Areán, E. Garrone and A. Zecchina, Catal. Lett. **61**, 187 (1999).
78. A. Zecchina, C. Otero Areán, G. Turnes Palomino, F. Geobaldo, C. Lamberti, G. Spoto and S. Bordiga, Phys. Chem. Chem. Phys. **1**, 1649 (1999).
79. G. Schmid, M. Bäumle, M. Geerkens, I. Heim, C. Osemann and T. Sawitowski, Chem. Soc. Rev. **28**, 179 (1999).
80. J. He, Y. Ba, C. I. Ratcliffe, J. A. Ripmeester, D. D. Klug, J.S. Tse and K. F. Preston, J. Am. Chem. Soc. **120**, 10697 (1998).
81. M. Ganschow, M. Wark, D. Wöhrle and G. Schulz-Ekloff, Angew. Chem. Int. Ed. **39**, 161 (2000).

Downloaded At: 12:22 15 January 2011

16. L. M. Bull, A. K. Cheetham, B. M. Powell, J. A. Ripmeester and C. I. Ratcliffe, J. Am. Chem. Soc. **117**, 4328 (1995).
17. J. M. Thomas, Stud. Surf. Sci. Catal. **93A**, 3 (1989).
18. R. F. Lobo, M. Pan, I. Chan, H. X. Li, R. C. Medrud, S. I. Zones, P. A. Crozier and M. E. Davis, Science **262**, 1543 (1993).
19. M. W. Anderson, O. Terasaki, T. Ohsuna, P. J. O. Malley, A. Philippou, S. P. Mackay, A. Ferreira, J. Rocha and S. Lidin, Phil. Mag. **B71**, 813 (1995).
20. O. Terasaki and T. Ohsuna, Catal. Today **23**, 201 (1995).
21. S. Nicolopoulos, J. M. González Calbet, M. Vallet Regí, A. Corma, C. Corell, J. M. Guil and J. Pérez Pariente, J. Am. Chem. Soc. **117**, 8947 (1995).
22. C. Otero Areán, M. Letellier, B. C. Gerstein and J. J. Fripiat, Dev. Sedimentol. **35**, 73 (1982).
23. G. Engelhardt and D. Michel, High Resolution Solid State NMR of Silicates and Zeolites, Wiley, Chichester, 1987.
24. J. Klinowski, Annu. Rev. Mater. Sci. **18**, 189 (1988).
25. H. Koller, B. Burger, A. M. Schneider, G. Engelhardt and J. Weitkamp, Microporous Mater. **5**, 219 (1995).
26. A. L. Blumenfeld, D. Coster and J. J. Fripiat, J. Phys. Chem. **99**, 15181 (1995).
27. J. Fraissard and T. Ito, Zeolites, **8**, 350 (1988).
28. K. S. Smirnov, A. A. Tsyganenko and B. Staudte, Chem. Phys. Lett. **182**, 127 (1991).
29. V. B. Kazansky, Acc. Chem. Res. **24**, 379 (1991).
30. J. C. Lavalley, Catal. Today **27**, 377 (1996).
31. A. Zecchina and C. Otero Areán, Chem. Soc. Rev. **25**, 187 (1996).
32. L. M. Kustov, Topics Catal. **4**, 131 (1997).
33. H. Knözinger and S. Huber, J. Chem. Soc. Faraday Trans. **94**, 2047 (1998).
34. J.C. Bart and G. Vlaic, Adv. Catal. **35**, 1 (1987).
35. C. Lamberti, G. Turnes Palomino, S. Bordiga, A. Zecchina, G. Spanò and C. Otero Areán, Catal. Lett. **63**, 213 (1999).
36. A. Zecchina, S. Bordiga, G. Spoto, D. Scarano, G. Petrini, G. Leofanti, M. Padovan and C. Otero Areán, J. Chem. Soc. Faraday Trans. **88**, 2959 (1992).
37. J. W. Ward, in: Zeolite Chemistry and Catalysis, ed. J. A. Rabo, ACS Monograph No. 171, Washington DC, 1976.
38. H. Förster, in: Spectroscopic and Computational Studies of Supramolecular Systems, ed. J. E. Davies, Kluver Academic Publishers, Dordrecht, 1992.
39. J. Klinowski, Chem. Rev. **91**, 1459 (1991).
40. H. Pfeifer and H. Ernst, Annu. Rep. NMR Spectrosc. **28**, 91 (1994).
41. J. P. Amoreux, F. Bauer, H. Ernst, C. Fernández, D. Freude, D. Michel and U. T. Pingel, Chem. Phys. Lett. **285**, 10 (1998).
42. M. W. Anderson, J. R. Agger, D. P. Luigi, A. K. Baggaley and J. Rocha, Phys. Chem. Chem. Phys. **1**, 2287 (1999).
43. E. M Flanigen, H. A. Szymanski and H. Khatami, Adv. Chem. Ser. **101**, 201 (1971).
44. M. D. Baker, G. A. Ozin and J. Godber, Catal. Rev. Sci. Eng. **27**, 591 (1985).
45. E. Geidel, H. Boehlig, C. Peuker and W. Pilz, Stud. Surf. Sci. Catal. **65**, 511 (1991).
46. K. Krause, E. Geidel, J. Kindler, H. Förster and K. Smirnov, Vib. Spectrosc. **12**, 45 (1996).
47. S. M. Csicsery, Zeolites **4**, 202 (1984).
48. P. B. Weisz, Pure Appl. Chem. **52**, 2091 (1980).
49. W. W. Kaeding, J. Catal. **95**, 512 (1985).
50. P. Ratnasamy, F. P. Babu, A. J. Chandwadkar and S. B. Kulkarni, Zeolites **6**, 98 (1986).
51. G. Paparatto, E. Moretti, G. Leofanti and F. Gatti, J. Catal. **105**, 227 (1987).

Downloaded At: 12:22 15 January 2011

82. S. Dai, Y. Shin, Y. Ju, M. C. Burleigh, J.S. Lin, C. E. Barnes and Z. Xue, Adv. Mater. **11**, 1226 (1999).
83. S. R. Hall, C. E. Fowler, B. Lebeau and S. Mann, Chem. Comm. 201 (1999).
84. T. Asefa, M. J. MacLachlan, N. Coombs and G. A. Ozin, Nature **402**, 867 (1999).
85. J. M. Thomas, T. Maschmeyer, B. F. G. Johnson and D. S. Shephard, J. Mol. Catal. A **141**, 139 (1999).
86. A. Joy, S. Uppili, M. R. Netherton, J. R. Scheffer and V. Ramamurthy, J. Am. Chem. Soc. **122**, 728 (2000).
87. C. Otero Areán, G. Turnes Palomino, A. Zecchina, G. Spoto, S. Bordiga and P. Roy, Phys. Chem. Chem. Phys. **1**, 4139 (1999).
88. T. Chen, V. Engel, M. Heid, W. Kiefer, G. Knoop, A. Materny, S. Meyer, R. Pausch, M. Schmitt, H. Schwoerer and T. Siebert, Vib. Spectrosc. **19**, 23 (1999).
89. U. Emmerichs, S. Wontersen and H. J. Bakker, J. Opt. Soc. Am. B **14**, 1480 (1997).
90. M. Bonn, H. J. Bakker, K. Domen, C. Hirose, A. W. Kleyn and R. A. van Santen, Catal. Rev. Sci. Eng. **40**, 127 (1998).

Downloaded At: 12:22 15 January 2011